JOURNAL OF MATERIALS SCIENCE **36** (2001) 3721 – 3730

An electron microscopic study of nickel sulfide inclusions in toughened glass

J. C. BARRY
Centre for Microscopy and Microanalysis, The University of Queensland, Brisbane, QLD 4072, Australia
E-mail: barry@uqimagel.emc.uq.edu.au

S. FORD
Resolve Engineering, AMP Place, Level 28, 10 Eagle St. Brisbane, QLD 4000, Australia

It has been known since the early sixties that nickel sulfide inclusions cause spontaneous fracture of toughened (thermally tempered) glass, but despite the considerable amount of work done on this problem in the last four decades, failures still occur in the field with regularity. In this study we have classified (by viewing through a 60× optical microscope) inclusions into two groups, which are "classic" and "atypical" nickel sulfides. The "classics" look like the nickel sulfide inclusions found at the initiation-of-fracture of windows that have broken spontaneously. We have compared the structure and composition of the "atypical" inclusions with the structure and composition of the "classics". All of the "classic" and "atypical" nickel sulfide inclusions studied in this work were found to have a composition in the range of $Ni_{52}S_{48}$ to $Ni_{48}S_{52}$. Inclusions on the nickel rich side of stoichiometric NiS were found to be two-phase assemblies, and inclusions on the sulphur rich side of NiS were single phase. It had been proposed that the "atypicals" were passive, and of a different composition to the "classics". However, we found that the difference between passive and dangerous nickel sulfide inclusions was not a difference in composition but rather a difference in the type of material in the internal pore space. The passive's had carbon char in their internal pore space, whereas the pore space of dangerous inclusions contained Na_2O. The presence of Na_2O and carbon char with the inclusions indicates that the formation of the inclusions results from a reaction of a nickel-rich phase with sodium sulphate and carbon.

1. Introduction

It was found by Ballantyne [1] in the early sixties that nickel sulfide inclusions cause spontaneous fracture of toughened glass. It is an expansion in nickel sulfide inclusions located at the interior portion of toughened glass (which is in tension), which causes the glass to break [2]. Schaal and Pieckert [2] reported that for high-rise buildings clad with toughened glass usually less than 1% of windows fail, but in rare cases up to 8% of windows have failed because of spontaneous fracture.

Following on from Ballantyne's discovery of the nickel sulfide inclusions, a great deal of engineering and scientific work in the glass industry has been focussed on an attempt to understand the causes and effects of the precipitation of nickel sulfide in glass melts [3–10].

Wohlleben *et al*. [3] found that the nickel sulfide inclusions in glass had a composition of $Ni_{1-x}S$. $Ni_{1-x}S$ is known to undergo a phase transformation at 379°C [11]. The transformation from the high temperature (hexagonal) αNiS to the low temperature (rhombohedral) βNiS is accompanied by a volumetric expansion of 2.8%.

Kullerund and Yund [11] had found that the α-β inversion in $Ni_{1-x}S$ becomes increasingly sluggish with increasing Ni deficiency as compared to stoichiometric NiS. Merker [5] made a careful study of the α-β inversion in $Ni_{1-x}S$ and found that for exact 1 : 1 NiS the transformation takes 13 mins at 250°C, whereas for $Ni_{0.93}S$ the transformation takes hundreds of times longer. Merker suggested that inclusions with close to stoichiometric NiS would be the most dangerous and that off-stoichiometric inclusions may take so long to transform so as to never break the glass within the lifetime of the building.

Most workers have concentrated on the fracture associated with $Ni_{1-x}S$, which is a stable phase in the composition range of NiS to $NiS_{1.08}$ (as shown by the phase diagram in Kullerud and Yund [11]). However, Wagner [6] found that inclusions which provoke fracture occur in the composition range Ni_7S_6 to $NiS_{1.03}$. That is, fracture occurs with compositions ranging from Ni_7S_6 to NiS as well as for $Ni_{1-x}S$. Wagner found that

inclusions of compositions Ni_7S_6, NiS and $NiS_{1.03}$ are yellow-gold in colour, have a rugged surface texture, are non-magnetic, and can provoke fracture of toughened glass. Wagner also found inclusions composed of Ni_3S_2 or $Ni_3S_2 + Ni$. These inclusions have a grey metallic colour, have a smooth surface texture, and are magnetic. The Ni_3S_2 and $Ni_3S_2 + Ni$ inclusions do not cause spontaneous fracture.

Although the structure of the crystalline phases on the sulphur rich side of stoichiometric NiS have been well characterised, there has been some difficulty in the characterisation of phases in the range from Ni_7S_6 to NiS. Kullerud and Yund [11] found that Ni_7S_6 has two polymorphs (α and β), which are stable below 573°C. The $\alpha \rightarrow \beta$ transformation is sluggish, and the stoichiometric αNi_7S_6 is more reluctant to change to the β polymorph than any other member of the solid solution series (by contrast, the NiS stoichiometric phase has the least sluggish $\alpha \rightarrow \beta$ transformation). βNi_7S_6 in equilibrium with NiS inverts at between 399°C and 401°C. The α form has an orthorhombic structure, whereas the β form was not indexed.

Seim *et al*. [12] developed a more up-to-date phase diagram for nickel sulfides which has the Ni_9S_8 phase in place of βNi_7S_6. For compositions on the nickel-rich side of stoichiometric NiS the Seim *et al*. phase diagram has a two-phase system with $\alpha Ni_{7+x}S_6 + Ni_{1-x}S$ at high temperature (below 577°C) converting to $Ni_9S_8 + NiS$ at below 387°C.

The crystal structure of αNi_7S_6 is given by Fleet [13] with density of 5.36 $g \cdot cm^{-3}$. The structure of Ni_9S_8 ($=\beta Ni_7S_6$) is given by Fleet [14] with a density of 5.273 $g \cdot cm^{-3}$. On the basis of differences in densities the transformation from αNi_7S_6 to Ni_9S_8 will cause an expansion of 1.6%. Since both the $\alpha \rightarrow \beta$ NiS and the $\alpha Ni_7S_6 \rightarrow Ni_9S_8$ transformations give rise to expansion it is no surprise that inclusions in the composition range from Ni_7S_6 to NiS cause spontaneous fracture, as was found by Wagner [6].

Wagner [6] suggests that if nickel sulfide forms within the glass melt then it is most likely to have a composition of Ni_3S_2. Further, Wagner suggests that NiS is formed by an oxidation step where,

$$Ni_3S_2 + 1/2O_2 \rightarrow NiO + 2NiS$$

Following this reaction the nickel oxide is dissolved in the glass so that the nickel sulfide is progressively enriched in sulphur.

There is a bit of a problem with Wagner's proposal in that the temperature in the glass tank ranges from 1100°C to 1400°C, whereas Rosenqvist [15] has shown that the partial pressure of S_2 over NiS is 1 atm at 850°C. This means that NiS of 1 : 1 stoichiometry should dissociate at above 850°C. The PS_2 is much lower for the more nickel rich phases. In order to survive at temperatures in the range 1100°C to 1400°C the inclusion would have to be at least as nickel rich as Ni_3S_2.

The sulphur is added to the melt in the form of sodium sulphate (a fining agent), but where does the nickel come from? Wagner [6] points out that the amount of sulphur in the burnt fuel oil alone could account for as much as 15 g of nickel per tonne of glass. There is only one nickel sulfide stone (which weighs about 5 μg) per tonne of glass, so that 15 g per tonne is more than 10^6 times as much nickel as is required to make the NiS stone. Wagner suggested that on combustion of the fuel oil the majority of the burn residue would be carried away by the recuperators but some of it may be deposited on the fire bricks, and that deposit may contain as much as 10% NiO. These deposits could be peeled off by the hot air and dropped into the glass tank. The high local concentration of nickel so produced could result in the formation of nickel sulfide.

Nickel-sulfide-inclusion-generated glass failure has been known about for almost four decades, and much work has been done. Even so, until quite recently, the work done had not brought forth any satisfactory solution to the problem since failures still occur in the field with regularity.

Apart from the need to understand the behaviour of nickel sulfide in the glass melt there is a need to find nickel sulfides in the windows before those windows fail. In Brisbane a partnership was formed between the University of Queensland and Resolve Engineering to find a way of detecting nickel sulfides in windows. The process developed by that partnership, which is known as the "photoglass" process [16, 17], was successfully used to find windows which contained nickel sulfide inclusions. The windows with the inclusions were then removed.

Of the windows removed some contained what we called "classic" nickel sulfides. These were inclusions which, when viewed through a 60× optical microscope, were seen to have a yellow-gold lustrous colour, a rugged surface texture, and a close to spherical shape. These inclusions have a surface texture which is somewhat similar to that of a golf ball. For many of the "classic" nickel sulfides there are prominent cracks in the glass adjacent to the inclusion. These inclusions were referred to as "classic" because they had an appearance which is quite similar to the appearance of inclusions found at the initiation-of-fracture of failed windows. Other windows that were removed contained what we called "atypical" nickel sulfide inclusions. These were inclusions that had the same yellow-gold colour as the "classics" but either had a smoother surface texture, or were prolate spheroids (football shape) rather than perfect spheres.

The motivation for this present study was to compare the structure and composition of the "atypical" nickel sulfide inclusions with the composition and structure of the "classic" nickel sulfides, and to compare both sets of inclusions from the intact windows with inclusions found at initiation-of-fracture in failed windows. A knowledge of the structure and composition of the "atypical" nickel sulfide inclusions would be helpful for future commercial projects. If the "atypicals" turn out to be harmless it will be possible to reduce the number of windows that are removed.

In this work the windows removed from the building were broken and the "classic" and "atypical" nickel sulfide inclusions were collected. At the same time non-nickel-sulfide inclusions which were found in these windows were collected as well.

2. Experimental

Samples were studied by *s*canning *e*lectron *m*icroscopy (SEM) and by *e*nergy *d*ispersive X-ray *s*pectroscopy (EDS). The inclusions were prepared for insertion into the SEM in one of three ways.

Specimen preparation method 1. The nickel sulfide inclusion from initiation-of-fracture of broken glass usually remains embedded on the surface of one of the fracture dice (when toughened glass windows fracture they break into small blocky shapes which are referred to as fracture dice). We take the fracture dice which contains the nickel sulfide stone, and in an optical microscope carefully (using a toothpick) apply carbon paint to the glass surface around the nickel sulfide inclusion (to prevent charging in the SEM). The nickel sulfide itself is quite a good electrical conductor. The sample is mounted on an aluminium stub in readiness for insertion into the SEM.

Specimen preparation method 2. The fracture dice plus inclusion is mounted onto a stub with wax with the inclusion facing into the wax and the glass is polished down until the nickel sulfide inclusion comes to the surface. The sample is thereafter prepared for SEM in the same way as for method 1. This method can also be used in the case where the inclusion does not come to the surface of the fracture dice when the window was broken.

Specimen preparation method 3. We used the method of Dyakivskii *et al*. [18] which is to liberate the stone from the glass by dissolving the surrounding glass matrix with hydrofluoric acid (HF). Nickel sulfide is not attacked by HF. We attach a 3 mm copper slot grid to a glass slide with a smear of wax, drop the liberated NiS stone into the centre of the slot gid and fix it in place with araldite. After the araldite has set the copper grid is removed from the glass slide. The copper slot grid plus inclusion is then mounted onto a stub and polished so as to bring the inclusion to the surface. We then apply carbon paint to the region around the NiS stone.

All samples were studied by SEM imaging in both *s*econdary *e*lectron *i*maging (SEI) and *b*ackscatter *e*lectron *i*maging (BEI) modes. The SEM imaging was performed in either a JEOL 6400F or a Philips XL30. EDS spectra were collected on the JEOL 6400F using an Oxford ultra-thin-window (UTW) silicon EDS detector with Moran Scientific analysis hardware and software. The spectra were collected for specimen tilt = 19°, spot = 5, condenser aperture = 2, working distance = 14 mm. Spectra were collected for both 10 kV and 20 kV accelerating voltages. The spectra were collected until there was at least 20,000 counts in all major peaks. A sample of the mineral millerite was used as an EDS standard (millerite is stoichiometric NiS). The millerite sample was prepared by specimen preparation method 2.

3. Results and discussion

3.1. Types of inclusions

In this work a detailed SEM imaging and EDS study was made of 9 nickel sulfide inclusions which had been located in toughened glass windows. The results of this study is summarised in Table I. Five of the inclusions 19/91, 1/91, 13/92, 4/93 and GM01, were found at the initiation of fracture in windows which failed by spontaneous fracture. Two inclusions, 13-08 and 34-31, were found in intact windows, but these inclusions came to a surface of a fracture dice when the windows were deliberately broken by us. These two inclusions would be considered as dangerous because the glass broke at the position of the inclusion. Two inclusions, 31-31 and 26-08, were found in intact windows, and these inclusions remained enclosed within a fracture dice when the windows were deliberately broken. These inclusions would be considered to be passive (not dangerous) because the glass broke at a position away from the inclusion.

Inclusions 19/91, 1/91 and 4/93 were prepared for SEM observation by method 3. Inclusions 13/92, GM01, 31-31 and 26-08 were prepared by method 2. Methods 3 and 2 produce specimens with a flat polished surface. These two methods allow us to study the internal structure of the inclusions. In addition, because the surface is polished flat it is possible to obtain good quantitative EDS results from these specimens. Inclusions 13-08 and 34-31 were prepared by method 1. In method 1 the original (hemispherical) surface of the inclusion can be studied in the SEM. Because the surface of the inclusion prepared by method 1 is not flat, the EDS results are not quantitative.

TABLE I Summary of compositions of nickel sulfide inclusions

Inclusn.	Diam. (μm)	Compsn. region 1	Std. dev. of Ni/S ratio	Compsn. region 2	Std. dev. of Ni/S ratio	Average compsn.
19/91	105 × 110	$Ni_{48}S_{52}$	4.4%	—	—	$Ni_{48}S_{52}$
1/91	155 × 160	Ni_9S_8	2.9%	NiS	2.6%	$Ni_{52}S_{48}$
13/92	330 × 350	$Ni_{49}S_{51}$	1.2%	$Ni_{52}S_{48}$	1.0%	$Ni_{50}S_{50}$
4/93	220 × 170	NiS	1.9%	Ni_9S_8	1.4%	$Ni_{50}S_{50}$
GM01	120 × 130	$Ni_{51}S_{49}$	2.9%	Ni_7S_6	2.5%	$Ni_{52}S_{48}$
13-08*	390 × 410	$Ni_{52}S_{48}$	3.4%	$Ni_{55}S_{45}$	5.0%	$Ni_{55}S_{45}$
34-31*	230	NiS	3.5%	—	—	$Ni_{50}S_{50}$
31-31•	160 × 170	$Ni_{48}S_{52}$	1.5%	—	—	$Ni_{48}S_{52}$
26-08•	150 × 160	Ni_7S_6	3.0%	$Ni_{49}S_{51}$	2.8%	$Ni_{52}S_{48}$

* From intact window, inclusion came to the surface of dice on fracture

• From intact window, inclusion remained inside glass dice on fracture

3.2. Nickel sulfide inclusions from initiation of fracture

In analysis of the stoichiometry of the inclusions we compare the EDS nickel and sulphur peak ratios in the inclusions with the ratios found for the standard (millerite). For 10 kV accelerating voltage it is the ratios of sulphur-k and the nickel-l peaks, and for 20 kV it is the ratios of the sulphur-k and the nickel-k peaks that are compared. Fig. 1a and b show EDS spectra at 10 kV and 20 kV for the Millerite standard. At 10 kV the EDS nickel-L (at an X-ray energy of 0.85 keV) and sulphur-K (2.3 keV) peaks are of similar height, with the nickel-L peak being the stronger. The nickel-Kα peak (7.47 keV) is very weak in the 10 kV spectra. At 20 kV the EDS nickel-L, sulphur-K and nickel-Kα peaks are of similar height, with the sulphur-K peak being the strongest.

Because there are at least 20,000 counts in all major peaks, the statistical error ($\pm\sqrt{N}/N$), is 0.7% in each peak, which means that the expected standard deviation in the ratio of two peaks is 1.4% ($=2 \times 0.7\%$). In comparing results from the 10 kV with the 20 kV EDS spectra on the same position in an inclusion, we find that the results are within the 1.4% of each other, as expected.

Fig. 2 has SEM images of inclusion 1/91. Fig. 2a is a backscatter electron (BE) image. From the BE image it is clear that there are two phases within the inclusion. The brighter region is more nickel rich, and the darker region is more sulphur rich. By image analysis it was determined that the brighter region occupied 57%, and the darker region occupied 43% of the total. There are pores in the inclusion (the pores are seen as black in the BE image). The pores make up 9% of the inclusion.

EDS analysis of the brighter and darker regions in 1/91 reveal that the brighter region (region 1 in Table I) has a composition of Ni_9S_8, whereas the darker region (region 2 in Table I) has the composition of NiS. The standard deviation of the Ni/S ratio (Table I) which is 2.9% for region 1 and 2.6% for region 2 is higher than the 1.4% expected on the basis of statistical fluctuation. Although the compositions average to the stated values within each region, there is a true variation of stoichiometry within these regions. The average composition of the whole inclusion (57% $Ni_9S_8 + 43\%$ NiS) is $Ni_{52}S_{48}$. For the nickel rich side of NiS, separation into the NiS and Ni_9S_8 phases is exactly what might be predicted based upon the most recent nickel sulfide phase diagram [12].

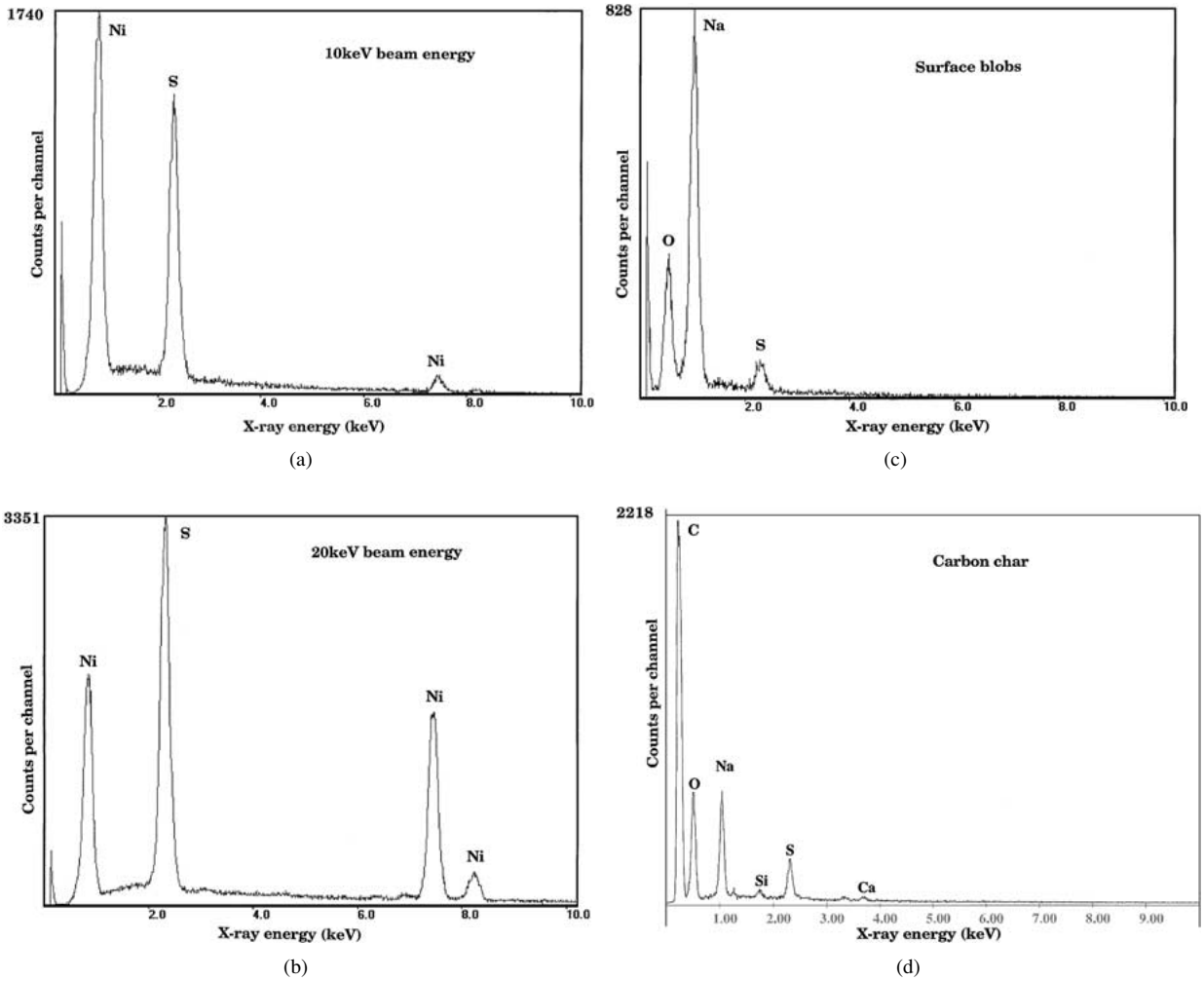

Figure 1 *E*nergy *d*ispersive X-ray *s*pectra (EDS). a) EDS of millerite (stoichiometric NiS) at 10 kV. The full-scale counts per channel is marked at the top left. b) EDS of millerite at 20 kV. c) EDS of black blobs on the surface of inclusion 34-31. These NaOH blobs are found on the surfaces of inclusions from freshly broken glass (see Fig. 5). d) EDS of carbon char from inclusion 31-31. Carbon char is found in the pore-space of the passive NiS inclusions (see Fig. 7).

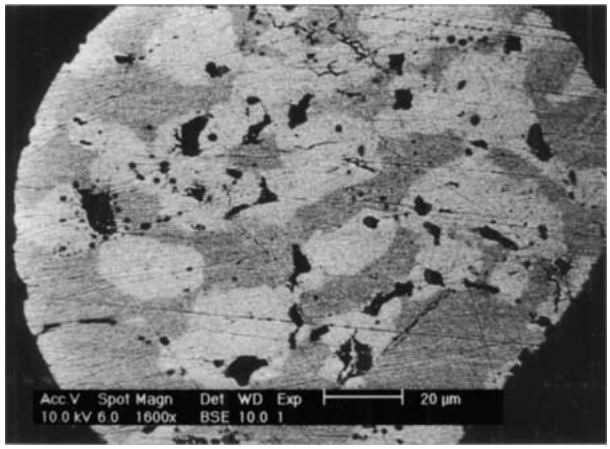

(a)

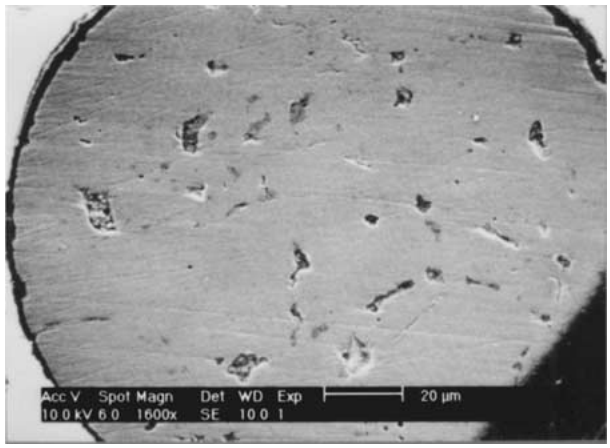

(b)

Figure 2 *B*ackscattered *e*lectron (BE) and *s*econdary *e*lectron (SE) images. a) BE image of inclusion 1/91. The brighter areas make up 57% of the whole. b) SE image of inclusion 1/91.

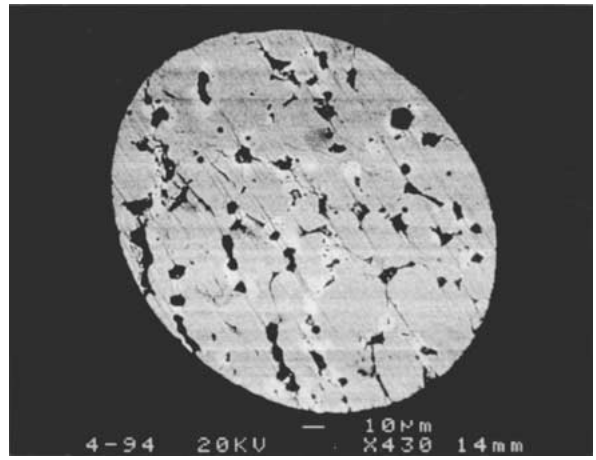

Figure 3 BE image of inclusion 4/93. The brighter areas only make up 6% of the whole.

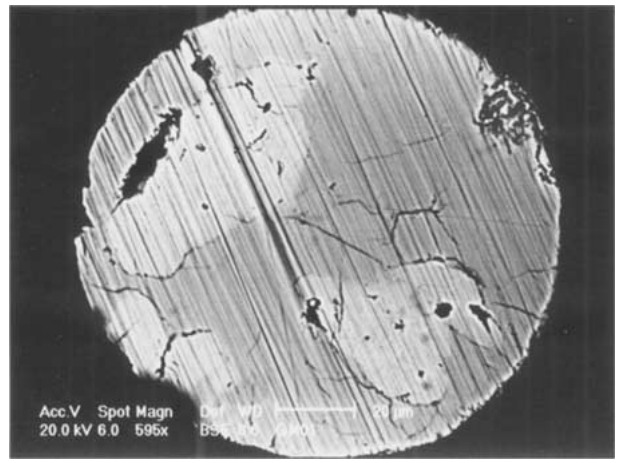

Figure 4 BE image of GM01. The brighter areas make up 28% of the whole.

A secondary electron (SE) image of 1/91 is shown in Fig 2b. In the SE image the structure of the pores may be seen more clearly. In the polished cross-sections the pores appear to be empty. EDS analysis of the inside surfaces of the pores indicate that these surfaces have the same composition as the adjacent polished section. Some of the pores do contain residue of the diamond polishing grit (as determined by EDS), but otherwise these pores appear to be empty.

Inclusion 4/93 also has two visible phases (Fig. 3). However, in the case of 4/93 the bright phase is very much in the minority with the darker phase being the dominant phase. The brighter regions in the BE image (Fig. 3) occupy only 6% of the total area, with the darker regions occupying the remaining 94%. The brighter regions occur in areas adjacent to the sample pores. EDS analysis of the two regions (summarised in Table I) shows that, as with 1/91, the brighter regions are the Ni_9S_8 phase and the darker region is the NiS phase. The average composition of the inclusion is $Ni_{50}S_{50}$. The pores make up 7% of the inclusion.

Inclusion 4/93 is rather elliptical in shape with an aspect ratio (=major axis divided by minor axis) of 1.3. All the other inclusions in this study were much more circular (spherical) in shape with aspect ratios of 1.05 or less. It had been suggested, anecdotally, that only spherical nickel sulfides break glass and that ellipsoidally shaped inclusions are not dangerous. Inclusion 4/93 came from the initiation-of-fracture of a broken window and it is clear that ellipsoidally shaped nickel sulfides inclusions must be considered as dangerous.

Inclusion GM01 (Fig. 4) also appears as a two phase assembly. However, the phases are not exactly the same as for 1/91 and 4/93. EDS analysis (Table I) reveals that the dark phase, which makes up 72% of the whole, has a composition of $Ni_{51}S_{49}$. The bright phase, which make up the remaining 28%, has a composition of Ni_7S_6. The average composition of the inclusion is $Ni_{52}S_{48}$. The pores make up only 2% of this inclusion. In Fig. 4 it can be seen that the inclusion was heavily scratched by the polishing media. Despite these polishing scratches, cracks within the inclusion are visible. It is interesting to note that in this inclusion many of the cracks follow the interface between the brighter and darker phases.

Of the other two inclusions which came from the initiation-of-fracture, 13/92 has two phases which are found by EDS to be $Ni_{49}S_{51}$ and $Ni_{52}S_{48}$, but 19/91 is single phase with a composition of $Ni_{48}S_{52}$ (Table I, images not shown). Since 19/91 is on the sulphur rich side of stoichiometric NiS we would expect it to have only a single phase. Inclusion 13/93 has 5% porosity. It was not possible to estimate the porosity of 19/91 because part of the inclusion pulled out of the polished surface.

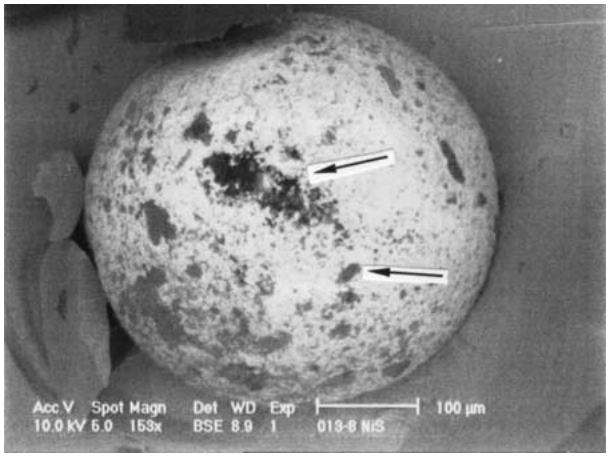

(a)

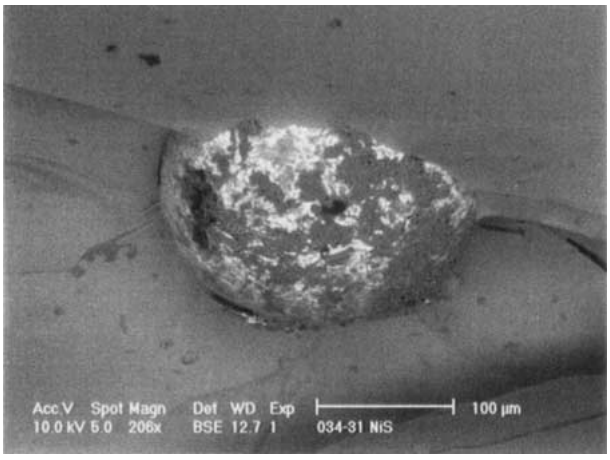

(b)

Figure 5 BE images of nickel sulfide inclusion surfaces. In the BE images the nickel sulfide appears white and the NaOH blobs on the surface appear black. a) Inclusion 13-08. The NaOH blobs are indicated by arrows. b) Inclusion 34-31.

3.3. Nickel sulfide inclusions from intact windows, where the inclusions came to the surface of fracture dice when the windows were deliberately broken

Two inclusions in this study, 13-08 and 34-31, were found embedded in the surfaces of fracture dice from windows which were deliberately broken. These inclusions were not polished or washed but rather were studied as is. The surface of the glass was painted with carbon paint to make an electrically conductive contact with the inclusions. BE images of inclusions 13-08 and 34-31 are shown in Fig. 5a and b. These inclusions have blobs on top of the nickel sulfide surface. In the BE images the blobs appear as black and the nickel sulfide surface appears as white.

When the surface of the inclusions is analysed, the part on the inclusion that appears white in the BE image is found to be nickel sulfide. However, when the black blobs are analysed we find only sodium and oxygen in the EDS spectra (Fig. 1c). The black blobs must be composed of sodium hydroxide, NaOH. Hydrogen is much too light to be detected by EDS; the EDS spectrometer will only detect from carbon upwards.

The black blobs (NaOH) on the nickel sulfide surface cover almost 50% of inclusion 34-31 (Fig. 5b). The inclusion was rotated so as to examine the profile (the edge-on view) of these surface blobs. By examination of the profile we estimate that the black blobs have a thickness of less that 3 μm. If we assumed that the NaOH were to cover 50% of inclusion 34-31 to a depth of 3 μm, then this material would make up only 1.3% of the total inclusion volume (the inclusion is 230 μm in diameter). Since the covering of NaOH is in fact less than 3 μm it follows that the NaOH on the surface makes up less than 1% of the inclusion volume. On inclusion 13-08 the black blobs cover only 15% of the surface, and on this inclusion the NaOH would make up much less than 1% of the inclusion volume.

Having seen the NaOH in the scanning microscope we decided to look for it in the optical microscope. Under the 60× optical microscope NaOH could be seen of the surface of inclusion 34-31. In the optical microscope the NaOH appears as small translucent crystals. The appearance of NaOH on the surface of the nickel sulfide inclusions is a significant observation, the implications of which will be discussed further below.

Inclusions 13-08 and 34-31 were analysed by EDS (Table I), but because these have a spherical surface we cannot define a standard X-ray generation geometry and therefore the EDS analysis cannot be taken as quantitative.

Inclusions 13-08 and 34-31 have very smooth surfaces as compared with the "classic" nickel sulfides. Fig. 6 shows a BE image of inclusion 20/93. This inclusion has the "classic" nickel sulfide surface texture which is somewhat rough. Almost all nickel sulfides found at initiation-of-fracture have the kind of surface texture as shown by 20/93. Inclusion 20/93 was not analysed by EDS.

Before we broke the glass to retrieve inclusions 13-08 and 34-31 it was postulated that these inclusions may not be nickel sulfide because they had such a smooth surface texture. What we have found in analysing these two inclusions is that, not only are they nickel sulfide inclusions, but also they are potentially dangerous because they lie on the glass fracture surface.

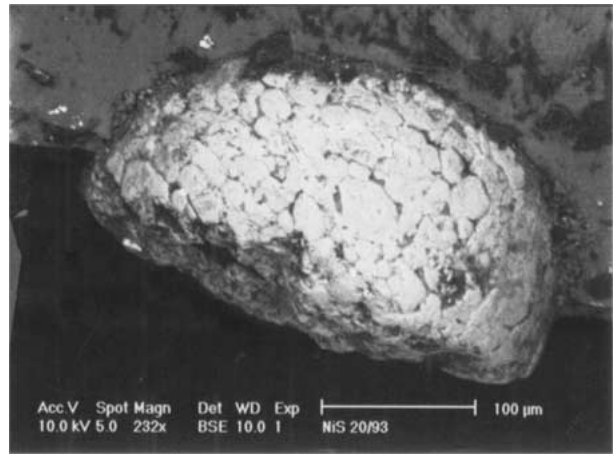

Figure 6 A BE image of inclusion 20/93. This inclusion has the "classic" nickel sulfide surface texture. The inclusion is 320 μm in diameter.

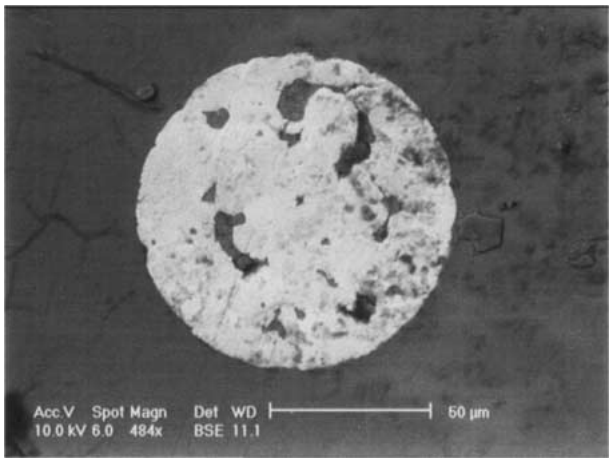

(a)

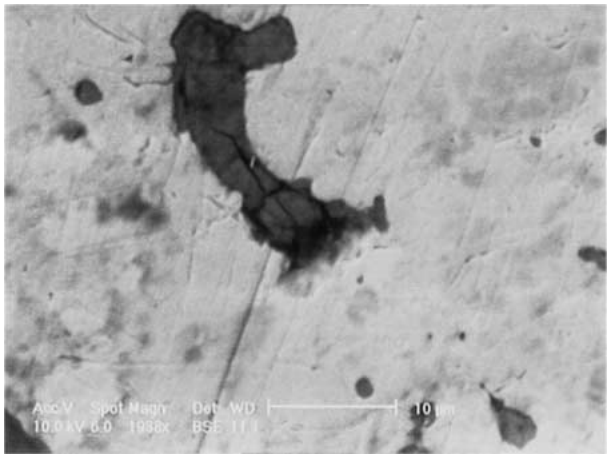

(b)

Figure 7 BE images of inclusion 31-31. a) An image of the whole inclusion. b) An image at higher magnification which shows that the pores are not empty.

3.4. Nickel sulfide inclusions from intact windows, where the inclusions remained inside the dice after fracture

The two inclusions in this study, 31-31 and 26-08, were found to remain inside fracture dice from windows which were deliberately broken. In order to try to make these inclusions come to a fracture surface, the dice containing the inclusion was heated and cooled by placing it in and out of a Bunsen burner flame. This heating and cooling process caused bits to break off the dice but did not bring the inclusions to the surface. Clearly these inclusions are quite passive.

A BE image of inclusion 31-31 is shown in Fig. 7a. The inclusion has 9% porosity, but as is shown more clearly in Fig. 7b, the pores are not empty. By EDS analysis the inclusion is found to be single phase (Table I) and has a composition of $Ni_{48}S_{52}$.

In inclusion 31-31 the major component of the material in the pores is carbon char (Fig. 1d), however, there are also small amounts of many other elements. The minor elements with the carbon char vary considerably from place to place. These elements include little or no nickel, but do include oxygen, sodium, iron, magnesium, silicon, sulphur and calcium.

Inclusion 26-08 is found to have 3.5% porosity (image not shown) and again the pores are not empty. By EDS analysis the inclusion is found to have two phases (Table I) which are Ni_7S_6 and $Ni_{49}S_{51}$. The average composition is $Ni_{52}S_{48}$. As with 31-31, in 26-08 the major component of the material in the pores is carbon char. The minor elements within the pore material are oxygen, nickel, iron, sodium, silicon, sulphur and calcium.

The passive inclusions 31-31 and 26-08 span the same composition range, from $Ni_{52}S_{48}$ to $Ni_{48}S_{52}$, as do the dangerous inclusions 19/1, 1/91, 13/92, 4/93 and GM01. The difference between the passive and non-passive inclusions has to do with whether the pores are empty or not. Although the dangerous inclusions were seen to have empty pores, we believe that those pores did originally contain a water soluble material. We prepared the inclusions from initiation-of-fracture by polishing them with diamond grit and rinsing with water. Any water soluble material would have been washed out.

We found NaOH on the surfaces of the freshly exposed inclusions 13-08 and 34-31 and we believe that while within the glass the inclusions would have had Na_2O on the surface and within the pores. The Na_2O would quickly convert to NaOH on exposure to the atmosphere. Any Na_2O in the pores would quickly wash out when the inclusions were rinsed after polishing.

We believe that the difference between the passive and dangerous inclusions is that the passive inclusions contain compressible carbon char in their pores while the dangerous inclusions contain incompressible Na_2O in their pores. When the nickel sulfide alpha to beta transformation occurs in the passive inclusion the expansion of the lattice may be taken up by crushing the carbon char, whereas with the dangerous inclusions the lattice expansion can only be accommodated through expansion of the whole inclusion. It is the expansion of the inclusion which cracks the glass in the tension zone and causes the windows to fail.

3.5. Inclusions and material in the glass other than nickel sulfide

A black shiny inclusion denoted BL31-31 was found in the same window as the nickel sulfide inclusion 31-31. A BE image of inclusion BL31-31 is shown in Fig. 8a. The inclusion appears to be a conglomerate of small grains. EDS analysis of the grains within the inclusion reveals that these grains are of two different types. The grains which appear brighter in the BE images are composed of sodium sulphate, that is, the EDS has oxygen, sodium and sulphur peaks. The grains that appear darker in the BE image are composed mainly of carbon char. There are minor elements in those grains as well as the carbon char. The minor elements with the carbon char are oxygen, sodium, magnesium, silicon, sulphur, potassium and calcium. It is interesting to note that the carbon char found in BL31-31 is similar in composition to the carbon char found in the pores of the nickel sulfide inclusions 31-31 and 26-08. The only significant difference between the carbon chars is that traces of nickel and iron are found in the pores of the nickel sulfide inclusions but are not found in BL31-31.

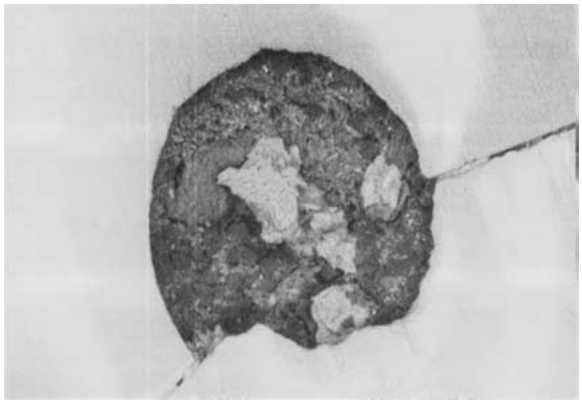

(a)

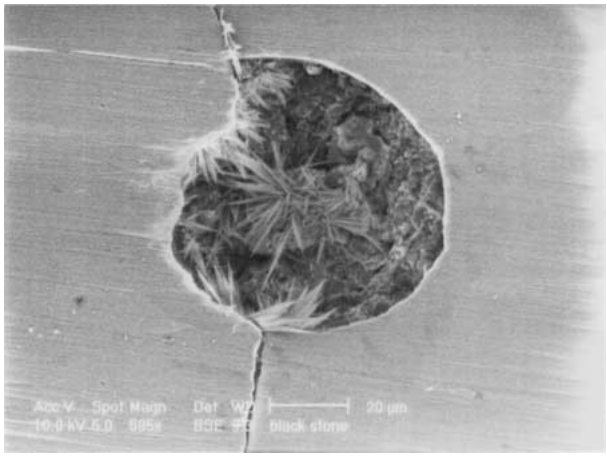

(b)

Figure 8 BE images of the non-nickel-sulfide inclusion BL31-31. a) An image soon after sample preparation. b) An image after the inclusion was exposed to the laboratory atmosphere for two months. Fibrous crystals have grown on the surface where sodium sulphate particles had been previously.

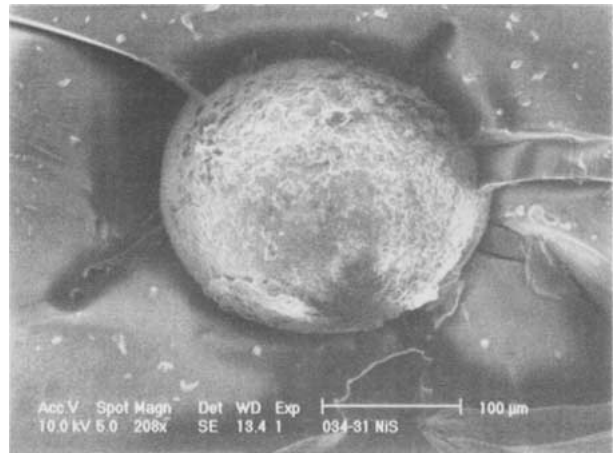

(a)

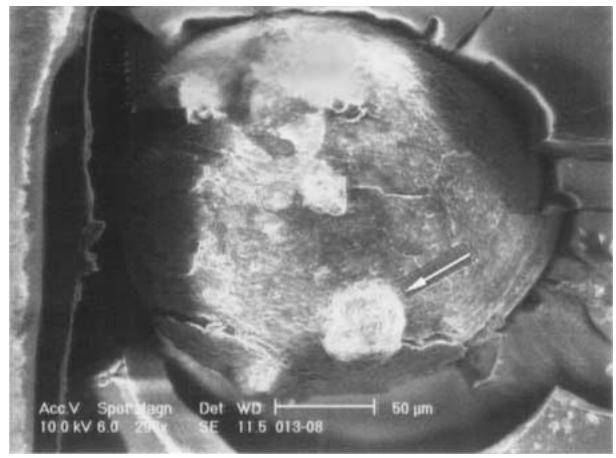

(b)

Figure 9 SE images of the nickel sulfide inclusion 13-08. a) An image taken within a week of glass fracture. b) An image taken after the inclusion had been exposed to the laboratory atmosphere for a few months. Some clumps of fibrous crystals (arrowed) have formed on the surface.

The carbon char and sodium sulphate found in inclusion BL31-31 would have been added with the initial charge. The sodium sulphate is added as a fining agent and the carbon is added as a reducing agent. The fact that these have survived the transit through the tank means that the glass melt must have maintained a reducing environment all the way through. In a reducing environment it is not surprising that nickel sulfide might survive in the glass melt, although at above 1000°C the nickel sulfide would have to be as Ni_3S_2 rather than as NiS.

An interesting thing happened to the material inside BL31-31 after the open inclusion had been left in the laboratory for two months. The laboratory is air conditioned so that the humidity would have been close to 60% and the temperature close to 22.5° at all times. Fig. 8b shows a BE image of BL31-31 after 2 months exposure to the laboratory atmosphere. Fibrous crystals have grown on the surface of the inclusion. The EDS of the fibrous crystals has peaks at oxygen, sodium, sulphur and calcium. The peaks heights vary somewhat from place to place on the fibres but the sodium peak is always at least twice as strong as the calcium peak. The places from where the fibres are growing were originally occupied by sodium sulphate. There was no calcium in the sodium sulphate region originally, although there was calcium in the surrounding carbon char. We believe that the fibres may be either glauberite ($Na_2Ca(SO_4)_2$) or glauber's salt ($Na_2SO_4 \cdot 10H_2O$) which arises as a result of hydration of sodium sulphate (Na_2SO_4).

The growth of crystals on the surface of BL31-31 was a bit of a surprise, but it turns out that such phenomena are not rare. It was found that the nickel sulfide 34-31 also had crystals growing on the inclusion surface after it had been in the laboratory for a few months. Fig. 9a shows a secondary electron (SE) image of 34-31 within a week of window fracture. Initially it was just a nickel sulfide inclusion with NaOH covering part of the surface. After a few months in the laboratory, as shown by the SE image of Fig. 9b, fibrous crystal are growing in clumps on the surface. The EDS on these crystals has major peaks at oxygen, sodium and sulphur, and has some very minor peaks at silicon, calcium, and nickel. It appears that the NaOH is reacting with the nickel sulfide inclusion and water vapour from the air to produce fibres of glauber's salt.

The observation of glauber's salt fibres growing on inclusion 34-31 has led us to examine optically some other nickel sulfides that we had in storage. When viewed through the 60× optical microscope these stored inclusions appear to have white furry stuff on their surfaces. The white furry stuff washes off in water and is most likely glauber's salt.

3.6. Possible reactions which lead to the formation of NiS in glass

As was stated in the introduction, the phase NiS is only stable at atmospheric pressure for temperatures of less than 850°C, and the stable phase in the glass tank (under reducing conditions) would be Ni_3S_2. We are led to the conclusion that although Ni_3S_2 must be forming in the glass melt tank, NiS can only form as the glass exits the melt tank and is being poured onto the hot tin. During the float-glass process, where the glass first makes contact with the tin, it is at 1000°C, and at the exit from the tin the temperature is 600°C [19]. The transit time of glass on the tin would be less than 30 seconds, and the time spent on the tin with a temperature less than 800°C would be less than 15 seconds. If we add the time of transit through the annealing lehr (after the glass comes off the tin), the total time that the glass temperature is below 800°C but is still reasonably hot (that is at around 600°C) is about 30 seconds. From this we conclude that the conversion from Ni_3S_2 to NiS takes less than 30 seconds.

But how does Ni_3S_2 convert to NiS? One possibility is that an inclusion such as BL31-31, which contained $NaSO_4$ and carbon, coalesces with a Ni_3S_2 inclusion and forms NiS by the following reaction:

$$Ni_3S_2 + Na_2SO_4 + 1\frac{1}{2}C \rightarrow 3NiS + Na_2O + 1\frac{1}{2}CO_2$$

If the above reaction were to happen we would expect about 25% of the inclusion to be composed of Na_2O. A point in favour of the above mechanism is that Na_2O is found on the surface of freshly exposed NiS inclusions, and we can postulate that there was originally Na_2O inside the pore space that is found in the dangerous inclusions. A point against the above mechanism is that the Na_2O found on the surface of the inclusion makes up only about 1-2% of the total volume, and the maximum pore volume found inside the inclusions was only 10% of the total. The maximum Na_2O volume in the dangerous inclusions could be no more than 12%, which is only half that predicted on the basis of the above mechanism.

A point in favour of the above mechanism is that the two passive inclusions studied, 31-31 and 26-08, had pores which contained carbon char. In the above mechanism, if not all the carbon were consumed, we would expect to retain carbon char inside the inclusion.

A point against the above mechanism is that it would be most unlikely that a Ni_3S_2 should meet a BL31-31 type inclusion just at the time that the glass is pouring out of the tank.

It may be instead that a coalescence of inclusions occurs inside the tank, which may be the coming together of a NiO and a BL31-31 type inclusion, with a reaction as follows:

$$3NiO + 2Na_2SO_4 + 3C \rightarrow Ni_3S_2 + 2Na_2O + 3CO_2$$

After this reaction some of the Na_2O may dissolve in the glass so that only a fraction of the Na_2O produced remains with the inclusion. On pouring the glass onto the tin, as the glass cools, the inclusion may be enriched in sulphur by taking dissolved sulphur out of the surrounding glass so that:

$$2Ni_3S_2 + 2S_2 \rightarrow 6NiS$$

we think that this is a probable mechanism because it could happen within the short time that the glass transits the tin.

According to the phase diagram a Ni_3S_2 inclusion will be a molten droplet at above 800°C. It is somewhat surprising that most nickel sulfide inclusions found are very close to spherical in shape because these inclusions exist in a molten form at the moment when the glass is poured onto the tin and stretched out. It must be that the Ni_3S_2 has a very high surface tension so that it can maintain a spherical shape while the molten glass deforms around it.

4. Conclusions

Of the inclusions studied in this work all inclusions with a yellow-gold lustrous colour were found to be nickel sulfide with a composition in the range of $Ni_{52}S_{48}$ to $Ni_{48}S_{52}$. The "classic" nickel sulfide inclusions with a rugged surface texture, a close to spherical shape, and a yellow-gold lustrous colour were found to be nickel sulfide within the range specified above. The "classic" nickel sulfides were found to be dangerous in that they caused spontaneous fracture.

Some inclusions which had been classified as "atypical" nickel sulfide were also found to cause fracture. Inclusion 4/93 did cause spontaneous fracture even though it was classified as "atypical" because it had an elliptical rather than round shape. Inclusions 13-08 and 34-31 were classified as "atypical" because they had a smooth rather than rugged surface texture - but these inclusions did cause glass fracture.

The two passive inclusions found, 26-08 and 31-31, both had the yellow-gold lustrous colour, but their surface texture was smoother that the "classics". Inclusion 26-08, in particular, had a surface with a fine dimpled structure which was a bit like the "classic" surface texture except that the dimples were much finer than those on the surface of a "classic".

The significant difference between the passive inclusions and the dangerous inclusions was not a difference in composition but rather a difference in the type of material in the internal pore space. The passive's had carbon char in their internal pore space, and we were able to infer that the dangerous inclusions had Na_2O in their internal pore space. The significance of this observation is that even if it becomes possible to identify the exact composition of the inclusions *in situ*, by using micro-Raman or some other technique [20], the composition alone is not enough to identify which stones are dangerous.

All inclusions which have the appearance of the "classic" nickel sulfide must be considered dangerous. Some of the "atypical" nickel sulfide inclusions are also dangerous. The "atypical" inclusions which have the rugged surface, but are not spherical, should

be treated as being the same as the "classics" since they are equally dangerous. Some "atypical" nickel sulfide inclusions which do not have a rugged surface texture may be passive. But others of the "atypical" nickel sulfide inclusions without the rugged surface texture do cause glass fracture, so that all "atypical" nickel sulfide inclusions should be considered as suspect, and windows containing those inclusions should be taken out of service.

Sodium hydroxide is found on the surface of nickel sulfide inclusions from freshly broken windows. This observation shows that the formation of the inclusions results from a reaction of a nickel-rich phase with sodium sulphate and carbon.

Acknowledgments

The authors would like to acknowledge the use of facilities at the Centre for Microscopy and Microanalysis, the University of Queensland. We would like to acknowledge the assistance of Barry Wood at the UQ Chemistry department and the glass examiners at Resolve Engineering for assistance in selecting the inclusions for this study. We would like to thank Gavin Miller for useful discussions of mineralogy issues.

References

1. E. R. BALLANTYNE, *CSIRO* "Division of Building Research" (Melbourne, Australia), Report No. 06, 1961, 1.
2. R. SCHAAL and W. PIECKERT, *Schweis. Alum. Rundich* **22** (1972) 383 (in French and German).
3. K. WOHLLEBEN, H. WOELK and K. KONOPICKY, *Glastech. Ber*. **39** (1966) 329 (in German).
4. H. TABUCHI, in Proc. of 10th International Congress on Glass, Kyoto (1974) Vol. 3 p. 54.
5. L. MERKER, *Glastechn. Ber*. **47** (1974) 116 (in German).
6. R. WAGNER, *ibid*. **50** (1977) 296 (in French).
7. M. V. SWAIN, *J. Mater. Sci*. **16** (1981) 151.
8. R. C. BRAND, *Advances in Ceramics* **22** (1988) 417.
9. J. C. BARRY, *Ultramicroscopy* **52** (1993) 297.
10. M. P. BRUNGS and X. Y. SUGENG, *Glass Technology* **36** (1995) 107.
11. G. KULLERUND and R. A. YUND, *J. Petrology* **3** (1962) 126.
12. H. SEIM, H. FJELLVÅG, F. GRØNVOLD and S. STØLEN, *J. Solid State Chem*. **121** (1996) 400.
13. M. FLEET, *Acta. Cryst*. **B28** (1972) 1237.
14. *Idem*., *ibid*. **C43** (1987) 2255.
15. T. ROSENQVIST, *J. Iron Steel Inst* **176** (1954) 37.
16. The Photoglass Process, http://www.resolve-eng.com.au/newtec.html
17. T. FORD, International Conference on Building Envelope Systems and Technology, University of Bath, April 1977.
18. S. I. DYAKIVSKII, V. I. KACHALIN and N. O. YAVORSKAYA, *Vestn. L'vov. Politekh. Inst*. **221** (1988) 92 (in Russian).
19. H. G. PFAENDER, "Schott Guide to Glass," 2nd ed. (Chapman Hall, London, 1996) p. 61.
20. D. W. BISHOP, P. S. THOMAS and A. S. RAY, *Materials Research Bulletin* **33** (1998) 1303.

Received 10 May 2000
and accepted 1 February 2001